X-ray scattering from interfacial roughness in multilayer structures

D. G. Stearns
University of California, Lawrence Livermore National Laboratory, P.O. Box 808, Livermore, California 94550

(Received 28 June 1991; accepted for publication 20 January 1992)

A quantitative theory of the nonspecular scattering of x rays from multilayer structures having rough interfaces is presented. The results are valid for arbitrary polarization and angles of incidence (measured from the normal) less than the critical angle for total external reflection. A structural model is adopted wherein each interface is assumed to be described by a surface having statistically random roughness with a well-behaved power spectrum. In addition, the model accounts for arbitrary correlation of the roughness between different interfaces. Calculations are presented for a variety of roughness configurations to investigate the dependence of the nonspecular scattering on the fundamental structural parameters. In particular, it is shown that the scattering from correlated roughness exhibits characteristic resonance behavior (quasi-Bragg diffraction).

I. INTRODUCTION

Thin films composed of synthetically grown multilayer (ML) structures represent a new class of materials having novel optical, electrical, magnetic, mechanical, and superconducting properties for a host of important applications. Since the interesting and unique properties of ML derive from the close proximity of different materials, it is not surprising that these properties are often strongly sensitive to the nature of the interfaces at the layer boundaries. In order to understand and control the physical behavior of ML, it is essential to be able to determine the detailed structure of the layers and interfaces, and to correlate this structure with the measured properties.

One important type of structural imperfection that can affect the properties of ML structures is interfacial roughness. For example, in electronic and magnetic ML,[1] interfacial roughness increases the amount of electron scattering by providing coupling to additional momentum states. In x-ray optical ML,[2] roughness both decreases the reflectivity and introduces a background halo that can degrade the resolution of imaging optics. There is also an increasing interest in understanding roughness as an intrinsic dynamic behavior of growing surfaces and interfaces. Recent theories[3–7] predict that the roughening of a surface follows simple scaling laws, and it has been shown[8] that ML structures can be useful experimental systems for studying the evolution of the surface roughness during film growth.

A promising technique for characterizing the roughness of surfaces and interfaces in ML structures is x-ray scattering. The use of x-ray scattering as a structural probe has several important advantages. It is inherently a noninvasive technique, well suited for dynamic measurements including *in situ* growth studies. The penetration of x rays allows both surfaces and buried interfaces as to be directly probed. Furthermore, due to the short wavelength of x rays, x-ray scattering can provide structural information on spatial scales ranging down to atomic dimensions. The roughness of single surfaces has been investigated using x-ray scattering,[9] and corresponding theoretical treatments applicable to a variety of conditions and approximations can be found in the literature.[10–13] More recently there has been increasing interest in using nonspecular x-ray scattering to study the roughness of multiple interfaces in ML structures. The first experimental results indicate that the x-ray scattering can exhibit a rich variety of behavior associated with the structural correlations between interfaces.[14–17] However, the interpretation of these results has been limited by the lack of a quantitative theory that incorporates realistic models of the interface structure. The goal of this paper is to present a simple theory that, within the limitations imposed by certain simplifying approximations, can provide a straightforward means of relating realistic interface structures to measurements of nonspecular scattering.

The scattering of radiation from multilayer optical coatings having rough boundaries has been considered previously. Early attempts[18,19] were directed at studying the effects of roughness on the specular scattering using scalar theory. Subsequently, Elson[20] developed a vector theory for the scattering of radiation from surface roughness, and applied the theory to ML coatings in which the roughness at the layer boundaries was either exactly reproduced from layer to layer (complete correlation) or was completely random at each layer (no correlation). Elson, Rahn, and Bennett[21] later extended the model to include a case where the roughness accumulates from the bottom to the top of the stack which corresponds to partial correlation. Bousquet, Flory, and Roche[22] developed a comprehensive theory of scattering from ML coatings that accomodates arbitrary correlations between the roughness of the different interfaces. Calculations based on this model have been compared to measured nonspecular scattering from multilayer optical coatings for the special cases of no correlation and complete correlation.[23] It is also possible to induce strongly correlated interface roughness in "ideal" ML coatings by applying surface acoustic waves. A purely kinematical description of x-ray scattering from such structures, assuming that the roughness is completely correlated, has been compared to experimental results.[24]

Most of this previous work was intended to describe

 0021-8979/92/094286-13$04.00

scattering from optical ML coatings at visible and near-ultraviolet wavelengths. Although the theoretical formalisms can in principle be applied to the scattering of x rays, we choose instead to apply the theory of the scattering of x rays from a nonideal ML structure developed in a previous paper[25] (referred to herein as Part I). This treatment utilizes the first Born approximation and hence is only valid under the condition that the scattering is weak and refraction can be neglected; that is, for incident and scattering angles (measured from the normal) less than the critical angle for total external reflection. At x-ray wavelengths the dielectric function is close to unity for all materials, so that even the specular (zeroth order) scattering is weak. Then for many experimental configurations this approximation is acceptable and offers the advantage of significantly simplifying the mathematical description of nonspecular scattering, particularly the term that Elson and Bennett[26] call the "optical factor" which accounts for the geometric and polarization effects.

In Sec. II we extend the results of Part I to treat the specific case of x-ray scattering from interfacial roughness in ML structures. A general model for interfacial roughness is introduced that can account for an arbitrary amount of correlation between layers. The model imposes no contraints on the power spectrum of the roughness, and thus is compatible with both conventional correlation-length-type and fractal-type descriptions of surface roughness.[27] The correlation of the roughness between layers is described by a frequency-dependent replication factor which can be used to either amplify or attenuate the roughness from layer to layer in a given frequency range. This represents an important extention of the earlier models for roughness propagation used in ML scattering theories, and is more consistent with the models currently used in theoretical treatments of surface roughening during film growth.

In Sec. III we present calculations of nonspecular scattering from a variety of different interface structures and configurations. In particular, we study the characteristic dependence of the scattering on structural parameters such as the number of layers, the root-mean-square roughness, the correlation length of the roughness, and the degree of correlation of the roughness between layers. Systematic variations in the nonspecular scattering are observed, including the appearance of resonance features (sometimes called "quasi-Bragg diffraction") when the interfacial roughness is correlated from layer to layer. The purpose of these calculations is to illuminate the close relationship between the nonspecular x-ray scattering and the detailed structure of the interfaces.

In Sec. IV we conclude by commenting on the implementation of the theory as it relates to the interpretation of experimental measurements.

II. THEORY

In Part I we presented a description of x-ray scattering from an interface of arbitrary structure. A special case is the scattering from a "slightly rough" boundary $f(x,y)$ between two media described by dielectric constants ϵ and ϵ'. As a review, we consider the configuration shown in Fig. 1. A plane wave, $\mathbf{E}_0\hat{\mathbf{e}}\exp(ik\hat{\mathbf{n}}\cdot\mathbf{x})$, propagating in direction $\hat{\mathbf{n}}$ with polarization $\hat{\mathbf{e}}$, is incident on the rough interface from above and scatters into direction $\hat{\mathbf{m}}$, experiencing a momentum transfer of

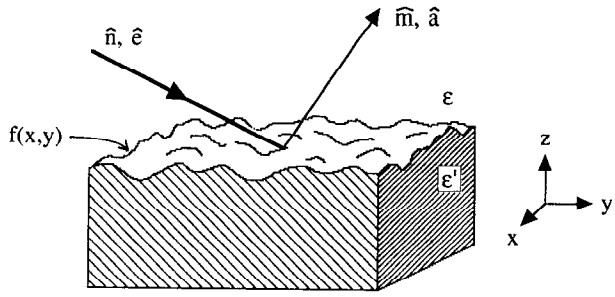

FIG. 1. The configuration of the radiation field scattered from a rough interface $f(x,y)$ separating two uniform media.

$$\mathbf{q} = k(\hat{\mathbf{m}} - \hat{\mathbf{n}}), \tag{1}$$

where k is the vacuum wave number. The difference in the dielectric constants of the two media $\Delta = \epsilon - \epsilon'$ is always small at x-ray wavelengths ($\Delta \ll 1$). Using the first Born approximation for the scattered field, the amplitude density of the field reflected into direction $\hat{\mathbf{m}}$ with polarization $\hat{\mathbf{a}}$ is given by

$$r(\hat{\mathbf{m}},\hat{\mathbf{a}};\hat{\mathbf{n}},\hat{\mathbf{e}}) = -i\mathbf{E}_0\frac{\Delta k^3}{8\pi^2 m_z}(\hat{\mathbf{a}}^*\cdot\hat{\mathbf{e}})\tilde{f}(s_x,s_y). \tag{2}$$

Here $\tilde{f}$ is the Fourier transform of f, $\mathbf{s} = s_x\hat{\mathbf{x}} + s_y\hat{\mathbf{y}}$ is the projection of $\mathbf{q}$ in the x-y plane, and $\hat{\mathbf{a}}^*$ represents the complex conjugate to account for the the case of circular polarization. It should be noted that the Born approximation is only valid when the scattering is weak and refraction of the transmitted field can be ignored, conditions that are generally satisfied for x rays when the incident and scattering angles (measured from the normal) are less than the critical angle for total external reflection. The Fourier transform in Eq. (2) results from the assumption that the interface is "slightly rough," such that

$$|q_z f(x,y)| = k(m_z - n_z)|f(x,y)| \ll 1 \quad \text{for all } x,y. \tag{3}$$

It is shown in Sec. II A that this condition is equivalent to requiring that the total integrated nonspecular scattering is small compared to the specular reflectance. We note that Eq. (3) is always satisfied when the interfacial roughness $|f(x,y)| \ll \lambda$, the x-ray wavelength.

The differential power dP_r reflected from an interface of area A into a solid angle $d\Omega$, per unit incident power, is given by

$$\frac{dP_r}{d\Omega}(\hat{\mathbf{m}},\hat{\mathbf{a}};\hat{\mathbf{n}},\hat{\mathbf{e}}) = \frac{4\pi^2 m_z^2}{n_z k^2 A}|r|^2. \tag{4}$$

Similarly, for a plane wave, $\mathbf{E}_0\hat{\mathbf{e}}\exp(ik'\hat{\mathbf{n}}\cdot\mathbf{x})$, incident onto the rough interface from below, the field amplitude density transmitted into direction $\hat{\mathbf{m}}$ with polarization $\hat{\mathbf{a}}$ is given by

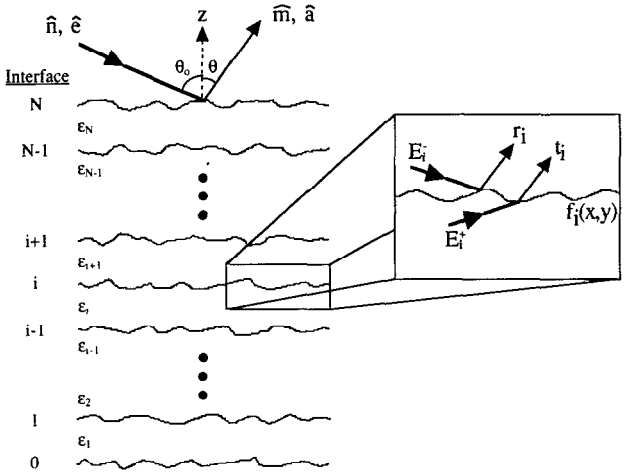

FIG. 2. Schematic diagram of a ML structure having rough interfaces. The inset shows the scattering at a particular interface, consisting of two contributions. The specular field incident from above and below the interface is scattered into the mode $(\hat{m},\hat{a})$ with amplitudes of r_i and t_i, respectively.

$$t(\hat{\mathbf{m}},\hat{\mathbf{a}};\hat{\mathbf{n}},\hat{\mathbf{e}}) = iE_0 \frac{\Delta k^3}{8\pi^2 m_z} (\hat{\mathbf{a}}^* \cdot \hat{\mathbf{e}}) \tilde{f}(s_x,s_y), \tag{5}$$

and the power scattered into that direction is

$$\frac{dP_t}{d\Omega}(\hat{\mathbf{m}},\hat{\mathbf{a}};\hat{\mathbf{n}},\hat{\mathbf{e}}) = \frac{4\pi^2 m_z^2}{n_z k^2 A} |t|^2. \tag{6}$$

Next consider the scattering from a multilayer stack consisting of a sequence $i = 1,2,...,M$ of layers having rough interfaces as illustrated in Fig. 2. The ith interface, defined as the boundary between layers i and $i+1$, is described by the surface $f_i(x,y)$. A plane wave of unit amplitude $\hat{\mathbf{e}} \exp(ik\hat{\mathbf{n}}\cdot\mathbf{x})$ is incident at an angle θ_0 on the top of the stack. For convenience, the propagation vector is chosen to have components of $n_x = 0$, $n_y = \sin\theta_0$, and $n_z = \cos\theta_0$, and the polarization $\hat{\mathbf{e}}$ is either S or P type. The propagation direction in the ith layer is altered by refraction to have the value $\hat{\mathbf{n}}^i$, where

$$\begin{aligned} n_x^i &= n_x, \\ n_y^i &= n_y, \\ n_z^i &= \frac{1}{|k_i|}\sqrt{k_i^2 - k^2 n_x^2 - k^2 n_y^2}. \end{aligned} \tag{7}$$

Here $k_i = |\epsilon_i^{1/2}| k$ and n_z^i is a complex quantity in the case of an absorbing medium.

The x-ray scattering within the ML structure is calculated using the specular field approximation, as discussed in Part I. In this approximation, the specular field in each layer is determined from a complete dynamical treatment of the specular scattering within the system of interfaces using well-known recursive[28] or matrix methods.[29] The Fresnel reflection coefficients can be modified to account for the interfacial roughness,[25] although this is required by condition (3) to be a small correction to the specular field.

Once the specular field in each layer is known, the nonspecular scattering is treated kinematically. The total nonspecular field is approximated as the sum of the fields scattered from each interface, taking into account extinction of the field as it propagates towards the top of the ML stack. We note that the kinematic treatment breaks down when the nonspecular scattering angle satisfies the ML Bragg condition, such that the multiple scattering exhibits constructive interference. This can either suppress or enhance the nonspecular scattering, in the same way that the specular transmission through a ML structure is modified at the Bragg condition.[25] Such distinctive features arising from multiple scattering of the nonspecular field have been experimentally observed.[15,16]

Let us consider the field scattered from the ML stack into the nonspecular direction $\hat{\mathbf{m}}$ with polarization $\hat{\mathbf{a}}$. As before, the propagation of the field in the ith layer is altered by refraction to be in the direction $\hat{\mathbf{m}}^i$. There are two contributions to the nonspecular field from each interface, corresponding to the scattering from the interface of the specular fields incident on either side (see Fig. 2). In particular, the specular fields incident on the ith interface from above and below are, correspondingly,

$$\mathbf{E}_i^-(\mathbf{x}) = E_i^- \hat{\mathbf{e}}^- \exp(ikn_y y)\exp(-ik_j n_z^j z) \tag{8}$$

and

$$\mathbf{E}_i^+(\mathbf{x}) = E_i^+ \hat{\mathbf{e}}^+ \exp(ikn_y y)\exp(ik_i n_z^i z), \tag{9}$$

where $j = i+1$ and the polarization $\hat{\mathbf{e}}^\pm$ corresponds to S or P type in accordance with the polarization of the incident field. The amplitudes of the specular fields, E_i^- and E_i^+, are determined using recursive or matrix methods as mentioned above. Each of these specular fields scatters from the rough interface, generating a nonspecular field that propagates towards the top of the stack. The incident field $\mathbf{E}_i^-$ scatters into mode $\hat{\mathbf{m}}^j$ with an amplitude density r_i given by Eq. (2),

$$r_i(\hat{\mathbf{m}}^j,\hat{\mathbf{a}};\hat{\mathbf{n}}^j,\hat{\mathbf{e}}^-) = -iE_i^- \frac{\Delta_i k_j^3}{8\pi^2 m_z^j} (\hat{\mathbf{a}}^* \cdot \hat{\mathbf{e}}^-) \tilde{f}_i(s_x,s_y), \tag{10}$$

where $\Delta_i = \epsilon_j - \epsilon_i$. Similarly, the incident field $\mathbf{E}_i^+$ scatters into mode $\hat{\mathbf{m}}^j$ with an amplitude density t_i given by Eq. (5),

$$t_i(\hat{\mathbf{m}}^j,\hat{\mathbf{a}};\hat{\mathbf{n}}^j,\hat{\mathbf{e}}^+) = iE_i^+ \frac{\Delta_i k_j^3}{8\pi^2 m_z^j} (\hat{\mathbf{a}}^* \cdot \hat{\mathbf{e}}^+) \tilde{f}_i(s_x,s_y). \tag{11}$$

The nonspecular field scattered from the ith interface accumulates phase as it propagates to the top of the ML stack. The phase contributed by traversal of the pth layer is defined as ϕ_p, given by

$$\phi_p = k t_p \sqrt{\epsilon_p - m_x^2 - m_y^2}, \tag{12}$$

where t_p is the thickness of the pth layer. The total phase accumulated upon reaching the vacuum interface at the top of the stack is $\Phi_i = \Sigma_{p=i+1}^{M} \phi_p$. The total amplitude density of radiation scattered into the vacuum in the direction $\hat{\mathbf{m}}$ is $\Sigma_{i=0}^{M} e^{\Phi_i}(r_i + t_i)$. Then, according to Eqs. (4) and (6), the scattered power is given by

$$\frac{dP}{d\Omega}(\hat{\mathbf{m}},\hat{\mathbf{a}};\hat{\mathbf{n}},\hat{\mathbf{e}}) = \frac{4\pi^2 m_z^2}{n_z k^2 A}\left|\sum_{i=0}^{M} e^{i\Phi_i}(r_i + t_i)\right|^2. \tag{13}$$

The theoretical development presented thus far is mostly a recapitulation of the results of Part I. Equation (13) describes the nonspecular scattering of x rays from a series of rough interfaces having completely arbitrary structures. To proceed we must adopt a specific model for the interfacial roughness in a ML stack. We postulate that the roughness of an interface can be separated into two components which we call the "intrinsic" and "extrinsic" parts. The intrinsic roughness $h(\mathbf{x})$, with the associated frequency spectrum $\tilde{h}(\mathbf{s})$, corresponds to that part of the interface structure that is inherent to the formation of the interface, and would be experimentally observed if the underlying interface was perfectly smooth. The extrinsic roughness corresponds to the structure derived from the replication of the roughness of an underlying interface. Hence the extrinsic roughness accounts for the propagation of roughness through the ML stack. It is reasonable that the extent of propagation varies with spatial frequency; components of roughness having wavelengths much longer than the layer thickness should be replicated, whereas the high-frequency components of roughness are likely to be planarized. To keep the model general we define a replication factor $\tilde{a}_i(\mathbf{s})$ which describes the fraction of the frequency component $\mathbf{s}$ in the $(i-1)$th interface that is replicated in the ith interface. Then the model for interfacial roughness in a ML stack can be written as

$$\tilde{f}_i(\mathbf{s}) = \tilde{h}_i(\mathbf{s}) + \tilde{a}_i(\mathbf{s})\tilde{f}_{i-1}(\mathbf{s}). \tag{14}$$

The first and second terms on the right-hand side represent the intrinsic and extrinsic roughness of the ith interface, respectively. The replication factor $\tilde{a}_i(\mathbf{s})$ can have any functional form, but is physically constrained to have the limiting values of unity and zero as $|\mathbf{s}|$ approaches 0 and ∞, respectively. By substituting recursively in Eq. (14) we obtain

$$\tilde{f}_i = \sum_{n=0}^{i} c_{in}\tilde{h}_n, \tag{15}$$

where

$$c_{in} \equiv \frac{\Pi_{m=0}^{i}\tilde{a}_m}{\Pi_{m=0}^{n}\tilde{a}_m}. \tag{16}$$

Equation (15) explicitly shows that the roughness of the ith interface is composed of its own intrinsic roughness $\tilde{h}_i$ and the intrinsic roughnesses $\tilde{h}_n$ of each of the underlying interfaces. The factor c_{in} represents the amount of intrinsic roughness inherited by layer i from the underlying layer n. The physical significance of the replication factor is made clear by taking the Fourier transform of Eq. (14) to obtain a description of the interface structure in real space,

$$f_i(\mathbf{x}) = h_i(\mathbf{x}) + a_i(\mathbf{x}) * [f_{i-1}(\mathbf{x})]. \tag{17}$$

The amount of roughness replicated from the underlying interface is determined by a convolution with the function $a_i(\mathbf{x})$. When $\tilde{a}_i(\mathbf{s})$ decreases monotonically with $|\mathbf{s}|$ then $a_i(\mathbf{x})$ decreases monotonically with $|\mathbf{x}|$, and the convolution serves to smooth the surface locally. This, of course, is the natural outcome of suppressing the replication of the higher-frequency components.

It is interesting to relate the model for the propagation of interfacial roughness in a ML structure to the theory of the roughening of the surface of a single film during growth. The difference equation (14), describing the roughness at a number of discrete interfaces, can be converted into a differential equation by considering the film, of total thickness t, as being composed of many thin layers having thickness Δt. We define the functions $\tilde{\eta}(\mathbf{s}) \equiv \tilde{h}(\mathbf{s})/\Delta t$ and $b(\mathbf{s}) \equiv [1 - \tilde{a}(\mathbf{s})]/\Delta t$, and take the limit of $\Delta t \to 0$ to obtain

$$\frac{\partial \tilde{f}(\mathbf{s},t)}{\partial t} = \tilde{\eta}(\mathbf{s}) - b(\mathbf{s})\tilde{f}(\mathbf{s},t). \tag{18}$$

If we let $b(\mathbf{s}) = 4\pi^2 \nu s^2$ then the Fourier transform of Eq. (18) yields the well-known Langevin equation describing the evolution of a growing surface derived by Edwards and Wilkinson,[3]

$$\frac{\partial f(\mathbf{x},t)}{\partial t} = \nu \nabla^2 f(\mathbf{x},t) + \eta(\mathbf{x}). \tag{19}$$

This is a differential equation representing isotropic diffusion in two dimensions, where the thickness of the film replaces the time variable. The first term on the right-hand side describes the relaxation of surface features due to a "diffusion coefficient" ν. The second term is a source term accounting for the introduction of random noise during growth. Kardar and co-workers[5] have pointed out that it is necessary to include a nonlinear term proportional to $(\nabla f)^2$ in Eq. (19) when the direction of growth is locally normal to the surface of the film. However, the behavior of the growth on sloped surfaces is likely to be strongly dependent on the detailed characteristics of the deposition process such as the collimation and energy of the incident adatoms, and it is not clear *a priori* whether the inclusion of a nonlinear term is more physically relevant. In any case, Eqs. (14) and (17)–(19) are linearized, lowest-order descriptions of roughness propagation in film growth, and are certain to be good approximations when the interface or surface slopes are small.

Having established a structural model for interfacial roughness in a ML, we proceed to develop an expression for the nonspecular x-ray scattering. We rewrite Eq. (13) as

$$\frac{dP}{d\Omega}(\hat{\mathbf{m}},\hat{\mathbf{a}};\hat{\mathbf{n}},\hat{\mathbf{e}}) = \frac{k^4}{16\pi^2 n_z A}\sum_{ij}(W_i W_j^* \tilde{f}_i \tilde{f}_j^*), \tag{20}$$

where the quantity W_i is defined by

$$W_i \equiv \Delta_i [E_i^+(\hat{\mathbf{a}}^* \cdot \hat{\mathbf{e}}^+) - E_i^-(\hat{\mathbf{a}}^* \cdot \hat{\mathbf{e}}^-)] e^{i\Phi_i}. \tag{21}$$

From Eq. (15) we have

$$\tilde{f}_i \tilde{f}_j^* = \left(\sum_{n=0}^{i} c_{in}\tilde{h}_n\right)\left(\sum_{l=0}^{j} c_{jl}\tilde{h}_l^*\right). \tag{22}$$

The intrinsic roughness $h_i(\mathbf{x})$ of each interface is statistically random, in the sense that it is completely uncorrelated with the intrinsic roughness of any other interface. Hence the phase of the quantity $\tilde{h}_n\tilde{h}_l^*$ has a random value, and every term in Eq. (22) for which $l \neq n$ vanishes when averaged over an ensemble of interface structures. This "random-phase approximation" is valid for measurements in which the spatial coherence length is much smaller than the dimensions of the x-ray beam, where the measurement averages over an ensemble consisting of different areas of the ML sample. However, in the case where the incident beam is spatially coherent, all of the terms in Eq. (22) will contribute to the scattered power, resulting in a varying and complex angular distribution analogous to the speckle patterns produced by the scattering of laser light from rough surfaces. Applying the random-phase approximation reduces Eq. (22) to

$$\tilde{f}_i\tilde{f}_j^* = \sum_{n=0}^{j} c_{in}c_{jn}\tilde{h}_n\tilde{h}_n^*, \quad j \leqslant i, = A \sum_{n=0}^{j} c_{in}c_{jn}\sigma_n^2 G_n. \tag{23}$$

where σ_n is the root-mean-square (rms) roughness defined as

$$\sigma_n^2 = \frac{1}{A}\int |h_n(\mathbf{x})|^2\, d\mathbf{x} = \frac{1}{A}\int |\tilde{h}_n(\mathbf{s})|^2\, d\mathbf{s} \tag{24}$$

and G_n is the normalized power spectrum of the intrinsic roughness h_n, defined as

$$G_n(\mathbf{s}) \equiv \frac{|\tilde{h}_n(\mathbf{s})|^2}{\int |h_n(\mathbf{s})|^2\, d\mathbf{s}}. \tag{25}$$

Finally, substitution of Eq. (23) into Eq. (20) yields

$$\frac{dP}{d\Omega}(\hat{\mathbf{m}},\hat{\mathbf{a}};\hat{\mathbf{n}},\hat{\mathbf{e}}) = \frac{k^4}{16\pi^2 n_z}\sum_{i=0}^{M}\left[\left(\sum_{n=0}^{i} c_{in}^2\sigma_n^2 G_n\right)W_iW_i^* + \sum_{j=0}^{i-1}\left(\sum_{n=0}^{j} c_{in}c_{jn}\sigma_n^2 G_n\right)\times(W_iW_j^* + W_i^*W_j)\right]. \tag{26}$$

This expression is the central result of the scattering theory, relating the power scattered by a ML consisting of M rough interfaces to the detailed structure of the interfaces. Each interface is characterized by fundamental structural parameters: the intrinsic rms roughness σ_n, the power spectrum $G_n(\mathbf{s})$ of the intrinsic roughness, and a set of replication factors c_{in}. The factors in parentheses containing G_n correspond to the structure factors in the language of x-ray-diffraction theory. All of the information relating to the structural configuration of the interfaces is contained in these factors. It is evident in Eq. (26) that the scattering separates naturally into two terms. The first term corresponds to the uncorrelated scattering, and is simply the sum of the intensities scattered by each interface independently. The second term corresponds to the correlated scattering. This contribution represents the interference of the radiation fields scattered by interfaces that have correlated structure due to the replication of roughness from layer to layer.

If the configuration of the surface roughness or the measurement geometry reduces to a one-dimensional scattering problem it is straightforward to show that Eq. (26) becomes,

$$\frac{dP}{d\theta}(\hat{\mathbf{m}},\hat{\mathbf{a}};\hat{\mathbf{n}},\hat{\mathbf{e}}) = \frac{k^3}{8\pi n_z}\sum_{i=0}^{M}\left[\left(\sum_{n=0}^{i} c_{in}^2\sigma_n^2 G_n^1\right)W_iW_i^* + \sum_{j=0}^{i-1}\left(\sum_{n=0}^{j} c_{in}c_{jn}\sigma_n^2 G_n^1\right)\times(W_iW_j^* + W_i^*W_j)\right], \tag{27}$$

where $G_n^1(s)$ is now the one-dimensional power spectrum of the intrinsic roughness of the nth interface.

Although Eq. (26) is a complicated result, it is quite general, valid for any ML structure that conforms to our model for propagating roughness. There are, however, several special cases for which the description of nonspecular x-ray scattering is considerably simplified.

A. Scattering from a single rough interface

In the case of scattering from a single rough interface described by a surface $h(\mathbf{x})$ having a rms roughness σ and a power spectrum $G(\mathbf{s})$, Eq. (26) reduces to

$$\frac{dP}{d\Omega}(\hat{\mathbf{m}},\hat{\mathbf{a}};\hat{\mathbf{n}},\hat{\mathbf{e}}) = \frac{k^4\sigma^2\Delta^2}{16\pi^2 n_z}|\hat{\mathbf{a}}^*\cdot\hat{\mathbf{e}}|^2 G(\mathbf{s}). \tag{28}$$

This is closely related to the bidirectional reflectance distribution function (BRDF), defined as $(n_z/m_z)dP/d\Omega$, which is used in optics to describe light scattering from a single surface.

Consider for the moment the special case where the nonspecular scattering is limited to an annular region near the specular direction. Then Eq. (28) can be approximated as

$$\frac{dP}{d\Omega} = \left(\frac{1}{\pi^2}\right)k^4\sigma^4 n_z^3 R_0 G(\mathbf{s}), \tag{29}$$

where

$$R_0 = \frac{\Delta^2}{16 n_z^4}|\hat{\mathbf{a}}^*\cdot\hat{\mathbf{e}}|^2 \tag{30}$$

is the specular reflectance from a perfectly smooth surface to lowest order in Δ, and $\hat{\mathbf{e}}$ and $\hat{\mathbf{a}}$ are the polarizations of the incident and specularly reflected fields, respectively. We use the relation $d\mathbf{s} = k^2 n_z\, d\Omega$ to write

$$dP(\mathbf{s}) = (1/\pi^2)k^2\sigma^2 n_z^2 R_0 G(\mathbf{s})\, d\mathbf{s}, \tag{31}$$

and integrate over all scattering vectors $\mathbf{s}$ to obtain an expression for the total integrated scattering (TIS) from the rough surface,

$$\mathrm{TIS} = (1/\pi^2)k^2\sigma^2 n_z^2 R_0 = (1/4\pi^2)q_z^2\sigma^2 R_0. \tag{32}$$

The TIS is equal to the decrease δR of the specular reflectance due to the surface roughness to lowest order in $q_z\sigma$ (neglecting scattering into evanescent modes). Applying the condition (3) which defines the case of "slight roughness," we arrive at an equivalent but more practical criterion defining the roughness limit,

$$\mathrm{TIS} = \delta R \ll R_0. \tag{33}$$

The roughness must be sufficiently slight so that the relative decrease in the specular reflectance from the ideal Fresnel reflectance is small.

When the limitations on the magnitude of the roughness are satisfied as discussed above, the description of nonspecular scattering from a single surface assumes a very simple analytic form. As an example, let the incident radiation be S polarized with an angle of incidence θ_0, and consider scattering into the S-polarization state in the direction (θ,ϕ) defined in spherical coordinates. Then Eq. (28) becomes

$$\frac{dP}{d\Omega}(\theta,\phi;\theta_0) = \frac{k^4\sigma^2\Delta^2\cos^2\phi}{16\pi^2\cos\theta_0}\,G(\mathbf{s}). \tag{34}$$

The power spectrum $G(\mathbf{s})$ is the Fourier transform of the normalized autocorrelation function $\gamma(\mathbf{x})$, defined by

$$\gamma(\mathbf{x}) \equiv \frac{\int h(\mathbf{u})h(\mathbf{u}+\mathbf{x})d\mathbf{u}}{\int |h(\mathbf{u})|^2\,d\mathbf{u}}. \tag{35}$$

If we assume that the interface is described by a spatially isotropic autocorrelation function having an exponential form,

$$\gamma(\mathbf{x}) = \gamma(r) = \exp(-r/L), \tag{36}$$

where $r = \sqrt{x^2+y^2}$ and L is the autocorrelation length, then the power spectrum is a Lorentzian,

$$G(s) = \frac{2\pi L^2}{(1+L^2s^2)^{3/2}}. \tag{37}$$

In the special case of normal incidence, where $s = k\sin\theta$, the power scattered by a single rough interface reduces to the particularly simple result,

$$\frac{dP}{d\Omega}(\theta,\phi;\theta_0=0) = \frac{k^4\sigma^2L^2\Delta^2}{8\pi\cos\theta_0}\,\frac{\cos^2\phi}{(1+L^2k^2\sin^2\theta)^{3/2}}. \tag{38}$$

This expression illustrates the general features of nonspecular x-ray scattering from interfacial roughness. The k^4 frequency dependence is characteristic of dipole scattering, where Δ corresponds to the magnitude of the dipole layer induced at the interface. The scattering into a direction θ is due to the coupling of the photon momentum with the component of interfacial roughness that has a frequency of $k\sin\theta$. The strength of the scattering is proportional to the magnitude of the power spectrum at that frequency. The factor $\cos\theta_0$ in the denominator is a geometrical factor that accounts for the change in the area of the interface illuminated by the incident beam. Finally, the factor $\cos^2\phi$ in the numerator represents the overlap of the incoming and outgoing polarizations.

B. Scattering from a ML having uncorrelated roughness

Next we consider the case of x-ray scattering from a ML consisting of M uncorrelated interfaces. Since there is no propagation of roughness, the replication factors are identically zero and the roughness of each interface is purely intrinsic,

$$\tilde{f}_i(\mathbf{s}) = \tilde{h}_i(\mathbf{s}). \tag{39}$$

It is easily shown that $c_{in} = \delta_{in}$ so that Eq. (26) reduces to

$$\frac{dP}{d\Omega}(\hat{\mathbf{m}},\hat{\mathbf{a}};\hat{\mathbf{n}},\hat{\mathbf{e}}) = \frac{k^4}{16\pi^2 n_z}\sum_{i=0}^{M}\sigma_i^2 G_i W_i W_i^*. \tag{40}$$

The scattering is simply a sum of the intensities scattered from each interface. The contributions are weighted by the factors $W_iW_i^*$ which contain information about the amplitude of the incident field at the buried interface, and the attenuation of the scattered field due to absorption. If the roughness of each interface is statistically equivalent, such that the rms roughness and power spectrum are identical, then

$$\begin{aligned}\frac{dP}{d\Omega}(\hat{\mathbf{m}},\hat{\mathbf{a}};\hat{\mathbf{n}},\hat{\mathbf{e}}) &= \frac{k^4\sigma^2 G}{16\pi^2 n_z}\sum_{i=0}^{M} W_iW_i^* \\ &= \frac{k^4\sigma^2\Delta^2 G}{16\pi^2 n_z}\sum_{i=0}^{M}\left|E_i^+(\hat{\mathbf{a}}^*\cdot\hat{\mathbf{e}}^+)\right. \\ &\quad \left. - E_i^-(\hat{\mathbf{a}}^*\cdot\hat{\mathbf{e}}^-)\right|^2.\end{aligned} \tag{41}$$

A comparison with Eq. (28) shows that the angular distribution of the scattered power is characteristic of the scattering from a single interface. We note that the scattering is proportional to the intensity of the specular field at the interfaces. When the specular field has a significant standing-wave component, such as near the Bragg condition in a periodic ML, the nonspecular scattering is modulated according to the relative position of the standing wave in the ML stack. The scattering is enhanced (suppressed) when the antinodes (nodes) of the specular field are located at the position of the interfaces.

C. Scattering from a ML having completely correlated roughness

Finally, we consider the case of x-ray scattering from a ML structure having M completely correlated interfaces. We assume that there is no intrinsic roughness ($G_i = 0$ for all $i \neq 0$), so that the roughness of each interface is an exact replication of the substrate surface $h_{\mathrm{sub}}(\mathbf{x})$. In this case the replication factors c_{in} are unity, and Eq. (26) reduces to

$$\begin{aligned}\frac{dP}{d\Omega}(\hat{\mathbf{m}},\hat{\mathbf{a}};\hat{\mathbf{n}},\hat{\mathbf{e}}) = \frac{k^4\sigma_{\mathrm{sub}}^2 G_{\mathrm{sub}}}{16\pi^2 n_z}\sum_{i=0}^{M}\Bigg(&W_iW_i^* \\ &+ \sum_{j=0}^{i-1}(W_iW_j^* + W_i^*W_j)\Bigg),\end{aligned} \tag{42}$$

where σ_{sub} and G_{sub} are the rms roughness and power spectrum of the substrate, respectively. The first term in the summation corresponds to the uncorrelated scattering

while the second term accounts for interference between the fields scattered at each interface. This interference term can either increase or decrease the nonspecular scattering for a given scattering angle and x-ray wavelength, depending on the phase relationship of the fields. If the fields scattered at each interface are phased such that they constructively interfere, then the double summation in Eq. (42) is approximately proportional to M^2 (assuming that extinction of the specular field in the ML is neglible). In this case the nonspecular scattering from completely correlated ML roughness can be as much as a factor of M stronger than the scattering from uncorrelated ML roughness.

III. MODELING THE NONSPECULAR SCATTERING FROM ML X-RAY OPTICAL COATINGS

As an example of the implementation of the theoretical results presented in the previous section, we have chosen to calculate the nonspecular scattering from ML structures designed as soft-x-ray optical coatings.[2] X-ray ML structures typically consist of alternating layers of high- and low-Z materials having individual layer thicknesses in the range of $\sim$10–100 Å. The reflectivity of the coating is optimized by choosing materials that (i) maximize the contrast in the index of refraction and (ii) minimize the absorption, which is always appreciable at soft-x-ray wavelengths. Examples of useful material combinations for normal incidence reflectivity are: Mo-Si (Ref. 30) for wavelengths greater than 124 Å (the Si L edge); Ru-B_4C (Ref. 31) for wavelengths greater than 65 Å (the B K edge); and W-C (Ref. 32) for wavelengths greater than 44 Å (the C K edge). Interfacial roughness in these ML is undesirable, as it degrades the x-ray optical performance by both decreasing the specular reflectivity and generating a diffuse background signal at the image plane due to nonspecular scattering. The detailed nature of the interfacial roughness varies with the materials system and can depend strongly on the growth conditions. Hence, a fundamental understanding of the growth and structure of the interfaces is important for improving the performance of ML x-ray optical coatings.

We have developed a code for simulating the nonspecular x-ray scattering from periodic ML structures commonly used as x-ray optical coatings. For the calculations presented in this paper, the ML is assumed to consist of alternating layers of Mo and Si separated by rough boundaries described by a set of surfaces $f_i(x,y)$. The thicknesses of the Mo and Si layers are t_{Mo} and t_{Si}, respectively, and the ML period is $\Lambda = t_{Mo} + t_{Si}$. The coating consists of a total of N layer pairs deposited on an infinitely thick Si substrate. We assume that the propagation of roughness in the ML is described by Eq. (14), and that all of the Mo-on-Si and Si-on-Mo interfaces are statistically equivalent. In particular, the intrinsic roughness of each type of interface is assumed to be random, isotropic in the x-y plane, and statistically represented by a rms roughness σ_i and autocorrelation length L_i, where the subscript i denotes an interface above a Mo layer (i = Mo), a Si layer (i = Si), or the substrate (i = sub). For convenience we use the exponential autocorrelation function and corresponding Lorentzian power spectrum given by Eqs. (36) and (37), respectively.

TABLE I. Values of the atomic scattering factors f_1 and f_2 and mass densities ρ used in the calculations of x-ray scattering from Mo-Si ML structures.

	f_1		f_2		ρ
	$\lambda = 10$ Å	$\lambda = 130$ Å	$\lambda = 10$ Å	$\lambda = 130$ Å	(g/cm^3)
Mo	35.7	14.4	8.6	2.1	10.2
Si	12.6	−3.1	0.74	0.46	2.33

Calculations of nonspecular x-ray scattering are presented for a variety of ML interface configurations relating to the three general categories of uncorrelated, correlated, and partially correlated roughness. In all cases the incident field consists of a monochromatic plane wave of wavelength λ, incident at an angle θ_0 with respect to the normal to the ML stack. The differential power scattered per unit incident power $dP/d\Omega$ is calculated as a function of the scattering angle θ in the plane of incidence ($\phi = 0$). The values used for the atomic scattering factors and the mass densities of Mo and Si are listed in Table I.

The limitations of the scattering theory restrict the calculations to cases where the scattered field is weak. As a simple guideline, we require that the field specularly reflected from an interface be at most one-tenth the strength of the incident field or, equivalently, that the x-ray reflectance of each interface be less than 1%. For example, the reflectance from a Mo-vacuum interface as a function of incident angle is plotted in Fig. 3 for x-ray wavelengths of 10 and 130 Å. The reflectance increases with increasing incident angle and reaches a value of 1% at incident angles of 85° and 55° for $\lambda = 10$ and 130 Å, respectively. We conclude that for Mo-Si ML structures, the condition of weak scattering is satisfied when the incident and scattering angles are restricted to a range of −85°–85° (−55°–55°) for $\lambda = 10$ Å ($\lambda = 130$ Å). As the x-ray wavelength decreases the critical angle for total external reflection (measured from the normal) generally increases,[33] and there is a corresponding increase in the angular range over

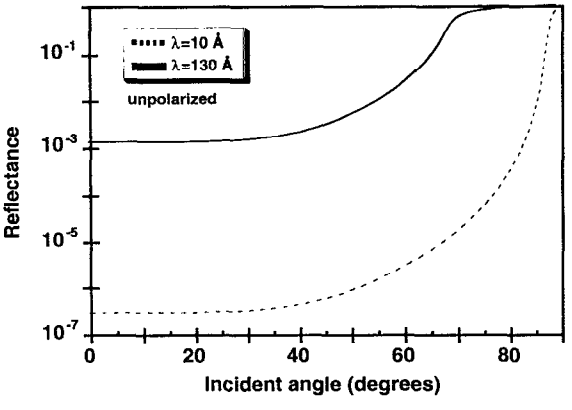

FIG. 3. Theoretical reflectance of a Mo vacuum interface as a function of incident angle for x-ray wavelengths of 10 and 130 Å.

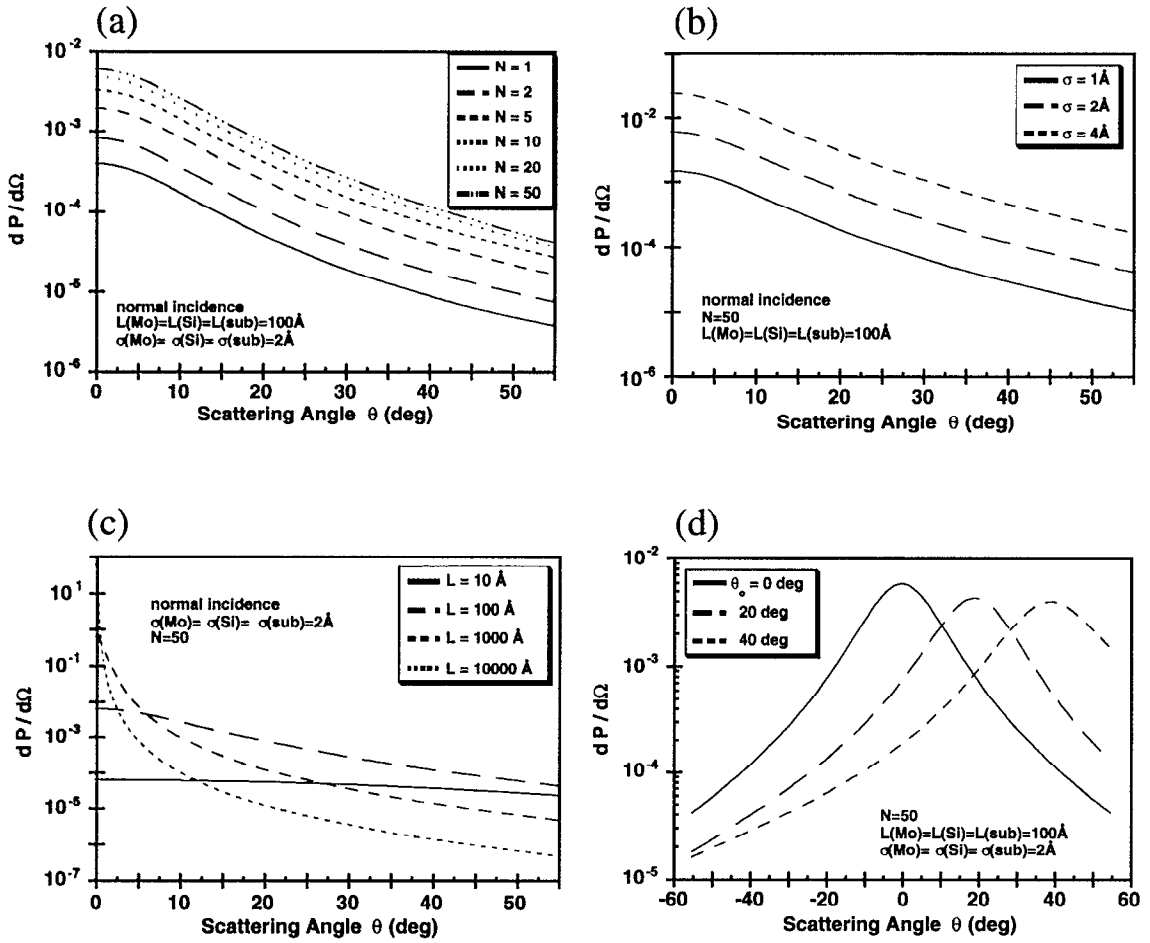

FIG. 4. Calculations of nonspecular x-ray scattering ($\lambda = 130$ Å) from a Mo-Si ML ($\Lambda = 75$ Å, $\Gamma = 0.4$) having uncorrelated interfacial roughness. Variation of the differential scattered power with (a) the number of ML periods, (b) the rms interfacial roughness $\sigma = \sigma_{\mathrm{Mo}} = \sigma_{\mathrm{Si}} = \sigma_{\mathrm{sub}}$, (c) the autocorrelation length $L = L_{\mathrm{Mo}} = L_{\mathrm{Si}} = L_{\mathrm{sub}}$ of the interfacial roughness, and (d) the angle of incidence.

which the scattering theory is valid. Hence the theory is well suited for describing the scattering of hard x rays ($\lambda \ll 1$ Å) from ML structures provided that the condition (3) for slight roughness is satisfied.

A. Uncorrelated roughness

In the case of uncorrelated roughness, as discussed in Sec. II B, the replication factors are identically zero so that there is no propagation of roughness through the ML stack. The roughness of each interface is purely intrinsic and is described by

$$\tilde{f}_i^{\mathrm{Mo,Si}}(s) = \tilde{h}_{\mathrm{Mo,Si}}(s), \tag{43}$$

where the power spectrum of f_i is given by Eq. (37). Figure 4 presents calculations of the nonspecular scattering from a ML having Mo and Si layer thicknesses of 30 and 45 Å, respectively. Unless otherwise stated, the angle of incidence is normal to the ML ($\theta_0 = 0°$) and the x-ray wavelength is $\lambda = 130$ Å.

The dependence of the x-ray scattering on the number of bilayers N in the ML stack is shown in Fig. 4(a). The different curves correspond to values of N ranging from 1 to 50. The interface parameters are $L_{\mathrm{Mo}} = L_{\mathrm{Si}} = L_{\mathrm{sub}} = 100$ Å and $\sigma_{\mathrm{Mo}} = \sigma_{\mathrm{Si}} = \sigma_{\mathrm{sub}} = 2$ Å. The scattered power is observed to roll off smoothly with increasing scattering angle, characteristic of the scattering from a single interface. As the number of layer pairs increases, there is a uniform, linear increase in the scattering intensity until approximately $N = 20$, where saturation is observed. Saturation occurs when the field amplitude inside the stack is attenuated due to specular reflection and absorption.

The dependence of the nonspecular scattering on the rms roughness parameter is shown in Fig. 4(b) for the case of $N = 50$ layer pairs. The rms roughnesses σ_{Mo}, σ_{Si}, and σ_{sub} are set equal and have values ranging from 1 to 4 Å. It is evident in Fig. 4(b) that the intensity of the scattering scales with σ^2 at all scattering angles, consistent with the dependence indicated by Eq. (26).

Calculations of the scattering for different values of the autocorrelation length ($L = L_{\mathrm{Mo}} = L_{\mathrm{Si}} = L_{\mathrm{sub}}$) in the range of $L = 10$–10^4 Å are presented in Fig. 4(c), where $N = 50$ and $\sigma_{\mathrm{Mo}} = \sigma_{\mathrm{Si}} = \sigma_{\mathrm{sub}} = 2$ Å. The angular distribution of the nonspecular scattering varies significantly with the autocorrelation length. When $L \ll \lambda$ the scattering is

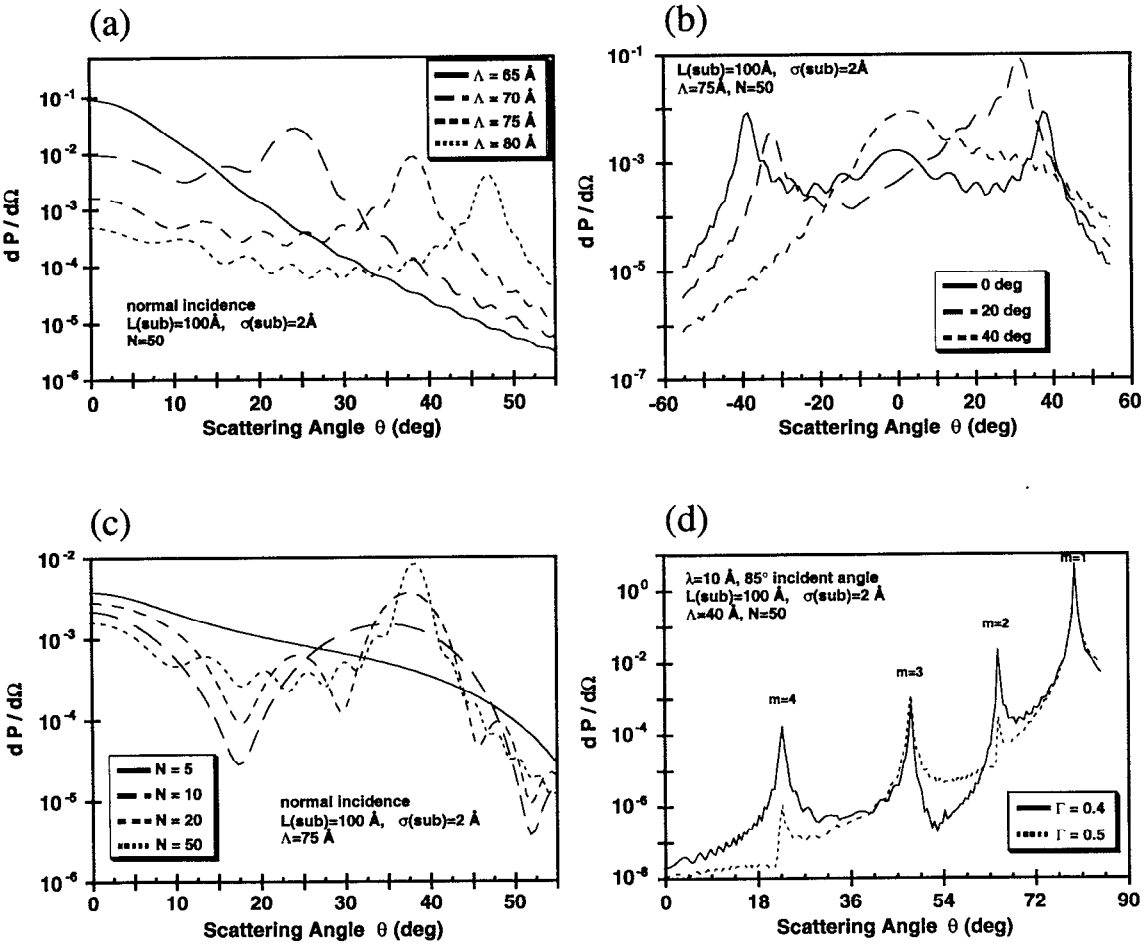

FIG. 5. Calculations of nonspecular x-ray scattering from a Mo-Si ML having complete correlation, where the roughness of the substrate is replicated exactly at each interface. Variation of the differential scattered power with (a) the ML period, showing resonant scattering at angles predicted by Eq. (45), (b) the angle of incidence, and (c) the number of ML periods. (d) Nonspecular scattering at $\lambda = 10$ Å from a ML having a period of $\Lambda = 40$ Å, for two values of the layer-to-thickness ratio Γ. Four distinct orders of resonant scattering are labeled.

fairly uniform with scattering angle. However, as L increases, the scattering becomes increasingly weighted in the specular direction ($\theta = 0°$). Of course, in the limit $L \to \infty$, the ML interfaces become perfectly smooth and the scattering is purely specular. The intensity of the scattering scales as L^2 at small θ, consistent with the L dependence of the power spectrum.

The nonspecular scattering for different angles of incidence ranging from $\theta_0 = 0°$–$40°$ is shown in Fig. 4(d). The interface parameters are $L_{\mathrm{Mo}} = L_{\mathrm{Si}} = L_{\mathrm{sub}} = 100$ Å and $\sigma_{\mathrm{Mo}} = \sigma_{\mathrm{Si}} = \sigma_{\mathrm{sub}} = 2$ Å. It is evident that the scattering always peaks in the specular direction, due to the maximum of the power spectrum at $s = 0$.

B. Correlated roughness

An essential feature of any model for ML interfacial roughness is the capability to account for the propagation of roughness through the ML stack. When propagation occurs, an interface is correlated with each of the underlying interfaces. The correlation of the interface structure provides a unique phase relationship between the radiation fields scattered from the interfaces, with a resulting profound effect on the nature of the scattered field. To illustrate this behavior we consider next the extreme case of complete correlation, where the replication factors are unity ($\tilde{a}_{\mathrm{Mo}} = \tilde{a}_{\mathrm{Si}} = 1$). Furthermore, we choose the ML interfaces to have no intrinsic roughness ($\sigma_{\mathrm{Mo}} = \sigma_{\mathrm{Si}} = 0$ Å). This yields the condition of purely extrinsic roughness considered in Sec. II C, where the surface profile of the substrate is exactly reproduced at each ML interface:

$$\tilde{f}_i^{\mathrm{Mo,Si}}(s) = \tilde{h}_{\mathrm{sub}}(s). \tag{44}$$

The roughness of the substrate is assumed to be described statistically by Eqs. (36) and (37) with an autocorrelation length of $L_{\mathrm{sub}} = 100$ Å and rms roughness of $\sigma_{\mathrm{sub}} = 2$ Å.

The calculated nonspecular x-ray scattering from a Mo-Si ML having completely correlated interfacial roughness is presented in Fig. 5. The scattering predicted for x rays at normal incidence and a wavelength of $\lambda = 130$ Å is shown in Fig. 5(a). The curves correspond to different values of the ML period in the range of $\Lambda = 65$–80 Å. In

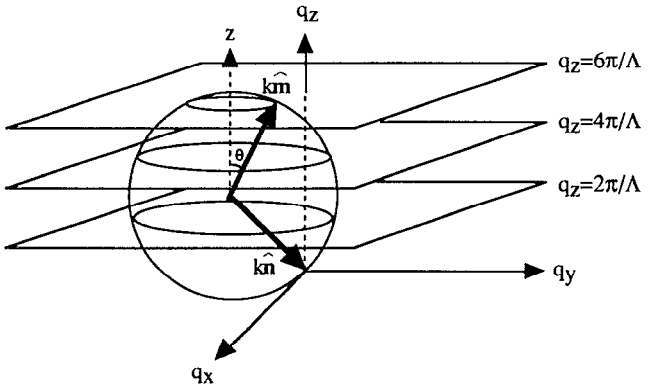

FIG. 6. Geometrical construction depicting the location of resonant nonspecular x-ray scattering in reciprocal space. Resonant scattering occurs wherever the sphere of radius k intersects the planes $q_z = 2\pi m/\Lambda$, corresponding to the set of circles defined in Eq. (46).

each case the ratio Γ of the Mo layer thickness to the ML period is kept at the constant value of 0.4. The scattering is characterized by a striking resonance surrounded by secondary oscillations. The angular position θ_p of the peak of the resonance is seen to vary systematically with the ML period. The origin of the resonance behavior can be understood by noting that the ML structure has a series of reciprocal lattice vectors along the z direction with magnitude $2\pi m/\Lambda$. The resonance in the nonspecular scattering occurs when the change in the momentum of the x ray along the z direction matches a reciprocal lattice vector of the ML, such that

$$|q_z| \approx \frac{2\pi m}{\Lambda}, \tag{45}$$

where $m = 1$ and $q_z = k\,(\cos\theta_0 + \cos\theta_p)$. Equation (45) neglects refraction corrections that are usually small at x-ray wavelengths. This is identical to the Bragg condition for x-ray diffraction from a ML, except that Bragg scattering requires that $q_x = q_y = 0$. The resonance behavior of the nonspecular scattering can be considered as quasi-Bragg diffraction, where a finite momentum transfer in the x-y plane is permitted.[14] As a result, the introduction of correlated roughness to a ML structure has an interesting effect in reciprocal space: The series of lattice points at $\mathbf{q} = (2\pi m/\Lambda)\hat{\mathbf{z}}$ corresponding to scattering from an ideal ML (i.e., having perfectly smooth interfaces) spread out into diffuse sheets located at $q_z = 2\pi m/\Lambda$. Then, for a given x-ray wave number k, the resonant nonspecular scattering is described by a circle in reciprocal space according to

$$(s_x + kn_x)^2 + (s_y + kn_y)^2 \cong k^2 - (2\pi m/\Lambda + kn_z)^2. \tag{46}$$

The conditions for resonant scattering expressed by Eq. (46) are illustrated in the geometrical construction presented in Fig. 6. The resonance scattering occurs along the sheets $q_z = 2\pi m/\Lambda$. The sheets have finite thickness δq_z given approximately by

$$\delta q_z \cong \frac{2\pi m}{N_{\text{eff}}\Lambda}, \tag{47}$$

where N_{eff} is the number of ML periods over which the roughness is correlated. For completely correlated roughness, N_{eff} is simply the total number of ML periods, independent of frequency. In the case of partially correlated roughness, where the correlation decreases at higher frequencies s, the sheets of resonant scattering become broader and more diffuse with increasing distance from the q_z axis. The x-ray scattering measurement at a particular wavelength λ interrogates points in reciprocal space that lie on a sphere of radius $k = 2\pi/\lambda$ having its center at the point $\mathbf{q} = -k\hat{\mathbf{n}}$ (the Ewald sphere). The intersection of this sphere with the planes at $q_z = 2\pi m/\Lambda$ are the set of circles defined by Eq. (46), representing the peak in the resonant scattering for a given experimental configuration (i.e., x-ray wavelength and incident angle). The angular position of the resonant scattering in real space is given by the direction of the circles with respect to the center of the sphere. From this construction it is clear that, for a given ML period Λ, an infinite series of scattering resonances are available; the number of orders m of resonant scattering that are experimentally accessible is determined by the x-ray wavelength (i.e., the radius of the Ewald sphere). The width of the resonance is determined by the thickness of the sheets as given by Eq. (47) and the trajectory of the scan in reciprocal space. Resonant nonspecular x-ray scattering of this type has been experimentally observed by several groups,[14–17] and some of the experimental issues are discussed by Savage *et al.*[15] The calculations presented in this paper correspond to "2θ" scans, where the incident beam is fixed and the detector position is varied.

Further examples of resonant scattering from a ML of period $\Lambda = 75$ Å are shown in Fig. 5(b). The different curves correspond to angles of incidence ranging from $\theta_0 = 0°$–$40°$. Scattering resonances occur in both the forward and backward directions, which corresponds to viewing a slice at $q_x = 0$ through the $m = 1$ circle of resonant scattering shown in Fig. 6. It is also apparent that the angular distribution of the scattering is weighted by the uncorrelated scattering distribution from a single interface; the scattering is enhanced in the specular direction.

The scattering of normal incidence x rays from a ML of period $\Lambda = 75$ Å having different numbers of layer pairs is presented in Fig. 5(c). The enhancement of the resonance behavior as the number of layer pairs increases is clearly evident. The intensity of the resonance peak scales as N^2 (until saturation occurs due to extinction of the incident field) and the frequency of the secondary oscillations increases with the number of layers. This behavior is typical of coherent scattering from a periodic structure (e.g., diffraction from multiple slits). The peak of the resonance corresponds to the condition where all of the fields are in phase; the maxima in the secondary oscillations occur at angles where the phase difference between the radiation scattered from the top and bottom interfaces is an integral multiple of 2π.

Resonant scattering from correlated roughness can oc-

cur whenever Eq. (46) is satisfied, resulting in a spectrum of harmonics associated with the different integer values of m. This behavior is illustrated in Fig. 5(d), where we show calculations of the scattering of unpolarized x rays at an incident angle of 85° and a wavelength of $\lambda = 10$ Å from a Mo-Si ML having $N = 50$ periods of $\Lambda = 40$ Å. The atomic scattering factors used in the calculation are listed in Table I. Four strong scattering resonances are clearly evident. The positions of the peaks are in good agreement with Eq. (46) and the corresponding values of m are labeled in the figure. The two curves represent different values for the ratio of the Mo layer thickness to the ML period: The solid and dashed curves correspond to values of $\Gamma = 0.4$ and 0.5, respectively. It is apparent that the even orders are suppressed when $\Gamma = 0.5$. This is because the fields scattered from the Mo-on-Si and the Si-on-Mo interfaces in each layer pair are π out of phase and hence destructively interfere. The same effect is observed for the diffraction orders of a ruled grating, where the even orders vanish when the line-to-space ratio is unity.

C. Partially correlated roughness

Although the cases of uncorrelated and completely correlated interfacial roughness are of interest for showing the limiting behavior of the x-ray scattering, it is unlikely that ML structures grown in the laboratory are well described by either of these extremes. A more realistic model for roughness propagation is the intermediate case of partial correlation, where the roughness of an interface includes a partial replication of the structure of the underlying interfaces. In the model (14) for ML interfacial roughness, the nature of the roughness propagation in the ML is dictated by the specific functional form of the replication factors $\tilde{a}_i(s)$. For the following calculations we use

$$\tilde{a}_i(s) = \frac{1}{1 + 4\pi^2 \nu_i t_i s^2}. \tag{48}$$

This form is chosen to be consistent with the linearized Langevin equation (19) for surface roughness propagation in the limit where the ML becomes a continuous film. In particular, the Hankel transform of Eq. (48) is

$$a_i(r) = \frac{1}{8\pi^3 \nu_i t_i} K_0 \frac{r}{2\pi \sqrt{\nu_i t_i}} \tag{49}$$

where $K_0(x)$ is the modified Bessel function having asymptotic values of $(-\ln x)$ as $x \to 0$ and $(x^{-1/2} e^{-x})$ as $x \to \infty$. Equation (49) is the solution for isotropic diffusion from a point source in two dimensions, where the thickness of the ith layer t_i substitutes for the time variable and ν_i is the diffusion coefficient. Hence for this specific choice of replication factor, the propagation of roughness behaves in a manner analogous to surface diffusion: A spike introduced at the $(i-1)$th interface propagates to the ith interface, annealing into a surface feature having a radius of $\sim \sqrt{\nu_i t_i}$. Correspondingly, a surface fluctuation of frequency s is damped to one-half of its original amplitude when the overlayer has a thickness of $t_i = 1/(4\pi^2 \nu_i s^2)$. The replication of roughness is strongly dependent on frequency; the low-frequency components of roughness tend to propagate more effectively through the ML stack, while the frequencies greater than $\sim 1/\sqrt{\nu_i t_i}$ are damped. Consequently, the correlation of the interfacial roughness between the different interfaces is greatest for the lower frequencies, and the x-ray scattering from the low-frequency components of the roughness is expected to exhibit the strongest resonant behavior.

With this particular model of roughness propagation, Eq. (14) becomes

$$\tilde{f}_i^{\mathrm{Mo,Si}}(s) = \tilde{h}_{\mathrm{Mo,Si}}(s) + \left(\frac{1}{1 + 4\pi^2 \nu_{\mathrm{Mo,Si}} t_{\mathrm{Mo,Si}} s^2}\right) \tilde{f}_{i-1}^{\mathrm{Si,Mo}}(s). \tag{50}$$

The total of eight parameters, $\sigma_{\mathrm{Mo,Si,sub}}$, $L_{\mathrm{Mo,Si,sub}}$, and $\nu_{\mathrm{Mo,Si}}$, in conjunction with the recursive relation (50), completely define the structure of the interfaces in the ML stack.

As an example, consider a ML structure in which the layers have no intrinsic roughness $[\tilde{h}_{\mathrm{Mo,Si}}(s) = 0]$. In this case the roughness at each interface is due solely to the replication of the roughness of the original substrate. If we assume that all of the layers have the same thickness Δt and value for the diffusion parameter ν, then from Eq. (50) the roughness of the ith interface can be written as

$$\tilde{f}_i(s) = \left(\frac{1}{1 + 4\pi^2 \nu \Delta t s^2}\right)^i \tilde{h}_{\mathrm{sub}}(s). \tag{51}$$

The interfacial roughness damps exponentially with the number of layers and the strength of the damping increases with increasing frequency. Taking the limit as $\Delta t \to 0$ and $i \to \infty$ yields an expression describing the roughening of a continuous film as a function of thickness t,

$$\tilde{f}(s;t) = \exp(-4\pi^2 \nu t s^2) \tilde{h}_{\mathrm{sub}}(s). \tag{52}$$

This is the solution of the differential equation (18) describing the diffusion of an initial perturbation $\tilde{h}_{\mathrm{sub}}(s)$ in the case where the source term $\tilde{\eta}$ vanishes.

Calculations of nonspecular x-ray scattering from a ML having partially correlated roughness ($\nu = \nu_{\mathrm{Mo}} = \nu_{\mathrm{Si}}$) are presented in Fig. 7. The structure of the Mo-Si ML is similar to the previous example ($\Lambda = 40$ Å, $\Gamma = 0.4$, $N = 20$), as is the incident field ($\lambda = 10$ Å, $\theta_0 = 85°$). Figure 7(a) shows the scattering for different values of the diffusion parameter ν in the case where the Mo and Si layers have no intrinsic roughness ($\sigma_{\mathrm{Mo}} = \sigma_{\mathrm{Si}} = 0$ Å). In this case, all of the interfacial roughness in the ML stack is due to replication of the substrate roughness characterized by $L_{\mathrm{sub}} = 100$ Å and $\sigma_{\mathrm{sub}} = 1$ Å. The four scattering resonances arising from the correlated roughness are clearly evident. Increasing the diffusion parameter ν causes the scattering intensity to decrease at all angles, as the interfacial roughness is damped more effectively. The damping is smallest at the scattering angles near the specular direction of $\theta = 85°$, which correspond to low-frequency components (i.e., smaller values of s).

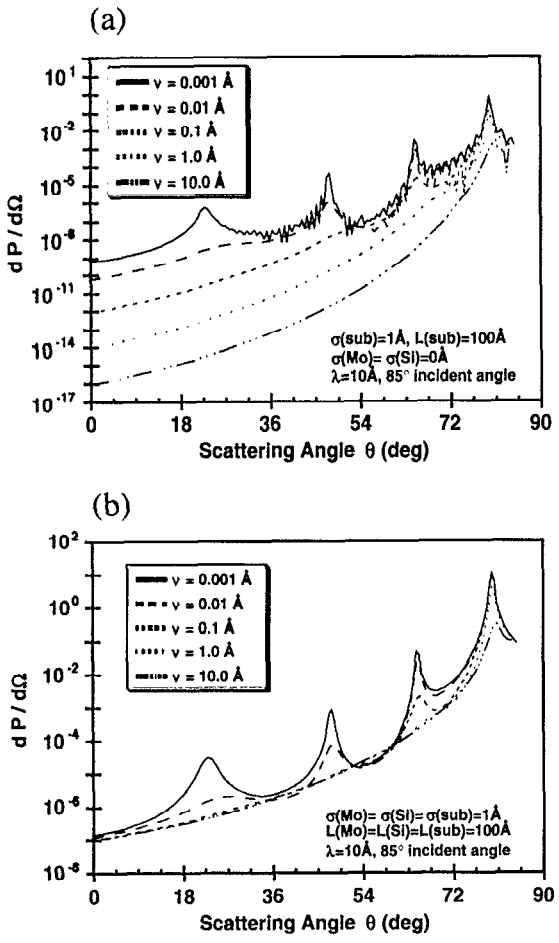

FIG. 7. Calculations of nonspecular x-ray scattering ($\lambda = 10$ Å) from a Mo-Si ML ($\Lambda = 40$ Å, $N = 20$, $\Gamma = 0.4$) having partially correlated roughness, for different values of the diffusion parameter $\nu = \nu_{Mo} = \nu_{Si}$. The differential scattered power is calculated for the cases of (a) no intrinsic roughness ($\sigma_{Mo} = \sigma_{Si} = 0$ Å) and (b) finite intrinsic roughness ($\sigma_{Mo} = \sigma_{Si} = 1$ Å).

We next allow the ML interfaces to include a component of intrinsic roughness. In this case, the roughness of the underlying layers is continuously damped, while new random roughness is introduced at each layer. After a number of layers has been deposited corresponding to a transient stage, the ML system converges to a steady-state condition where the roughness of the interfaces is constant. If we assume for simplicity that each of the $M = 2N$ interfaces is characterized by the same replication factor $\tilde{a}(s)$ and intrinsic roughness $\tilde{h}(s)$, then it is straightforward to show that the power spectral density (PSD) of the interfacial roughness converges to

$$\mathrm{PSD} \equiv |\tilde{f}(s)|^2 = \frac{1-\tilde{a}^{2M}(s)}{1-\tilde{a}^2(s)}\sigma^2 G(s) \rightarrow \frac{\sigma^2 G(s)}{1-\tilde{a}^2(s)}, \quad \text{as } M \rightarrow \infty, \tag{53}$$

where σ and $G(s)$ are the rms roughness and power spectrum associated with $\tilde{h}(s)$. This relationship provides a direct method of determining the intrinsic interface roughness from the PSD measured at any interface in the ML stack (e.g., the top surface).

An example of the nonspecular x-ray scattering from a ML that includes intrinsic roughness is presented in Fig. 7(b). X-ray scattering ($\lambda = 10$ Å, $\theta_0 = 85°$) from the Mo-Si ML considered previously ($\Lambda = 40$ Å, $\Gamma = 0.4$, $N = 20$) is calculated for the case in which the intrinsic roughness of all the layers (and the substrate) is identical: $L_{Mo} = L_{Si} = L_{sub} = 100$ Å, $\sigma_{Mo} = \sigma_{Si} = \sigma_{sub} = 1$ Å, and $\nu_{Mo} = \nu_{Si}$. The curves in Fig. 7(b) correspond to different values of the diffusion parameter ν. At small values of ν the scattering resonances due to correlated roughness are clearly visible. However, the introduction of intrinsic roughness entirely washes out the secondary oscillations. As ν increases, the replication of roughness from layer to layer is damped, thereby diminishing the amount of correlation. Correspondingly, the intensity of the scattering resonances decrease, and converge to a smooth background characteristic of the scattering from a ML having completely uncorrelated interfacial roughness. The sensitivity of the resonance structure on the diffusion parameter varies with the order of the resonance. The highest orders are suppressed rapidly with increasing ν since these correspond to scattering from the higher spatial frequencies.

IV. CONCLUSION

The theory presented in this paper provides a general framework for describing the nonspecular x-ray scattering from interfacial roughness in ML structures, valid within the limitations imposed by the following simplifying assumptions: (i) The scattered field is weak and refraction can be neglected, (ii) multiple scattering of the nonspecular field can be neglected, and (iii) the interfacial roughness is slight as defined by condition (3).

As in the case of x-ray diffraction from crystal lattices, the nonspecular scattering from roughness in a ML structure is often sufficiently weak to justify the neglection of refraction and multiple scattering. Within this kinematic approximation, the momentum transfer $\mathbf{q}$ of the scattered x ray maps to a single point in reciprocal space, and the intensity of the scattering at that point is directly related to the power spectra of the interfacial roughness through Eq. (26). The nonspecular x-ray scattering at measurable angles derives from those frequency components of the interfacial roughness having spatial wavelengths in the vicinity of λ, the x-ray wavelength. The smallest spatial wavelength that can be interrogated is $\sim\lambda/2$, corresponding to backscattering. The largest spatial wavelength that contributes to the nonspecular scattering is the projection of the transverse coherence length of the x-ray beam onto the surface of the ML sample. Thus a specific frequency regime in the power spectrum of the interfacial roughness can be studied by choosing an appropriate wavelength and configuration of the incident field.

The theory predicts a wide range of interesting phenomena, some aspects of which have been explored in the calculations presented in Sec. III. In particular, when roughness propagates through the ML, resulting in correlation between the structure of the different interfaces, in-

terference in the x-ray scattering produces a characteristic resonance behavior. This resonant scattering occurs at the locus of points in reciprocal space defined by the set of planes $|q_z| = 2\pi m/\Lambda$. By adopting the physically reasonable model for roughness propagation in a ML expressed by Eq. (14), we have established a quantitative relationship between the correlation of the interface structure and the resonant nonspecular scattering. The modeling of resonant scattering should provide a sensitive measure of the existence and degree of correlation in the ML interfacial roughness.

ACKNOWLEDGMENT

This work was performed under the auspices of the U.S. Department of Energy by Lawrence Livermore National Laboratory under Contract No. W-7405-ENG-48.

[1] B. Y. Jin and J. B. Ketterson, Adv. Phys. **38**, 189 (1989).
[2] E. Spiller, in *Physics, Fabrication, and Applications of Multilayered Structures*, edited by P. Dhez and C. Weisbuch (Plenum, New York, 1987), p. 271; E. Spiller, R. A. McCorkle, J. S. Wilczynski, L. Golub, G. Nystrom, P. Z. Takacs, and C. Welch, Opt. Eng. **30**, 1109 (1991).
[3] S. F. Edwards and D. R. Wilkinson, Proc. R. Soc. London Ser. A **381**, 17 (1982).
[4] R. Messier and J. E. Yehoda, J. Appl. Phys. **58**, 3739 (1985).
[5] M. Kardar, G. Parisi, and Y.-C. Zhang, Phys. Rev. Lett. **56**, 889 (1986); E. Medina, T. Hwa, M. Kardar, and Y.-C. Zhang, Phys. Rev. A **39**, 3053 (1989).
[6] C. Tang, S. Alexander, and R. Bruinsma, Phys. Rev. Lett. **64**, 772 (1990).
[7] H. Yan, D. Kessler, and L. M. Sander, Phys. Rev. Lett. **64**, 926 (1990).
[8] D. J. Miller, K. E. Gray, R. T. Kampwirth, and J. M. Murduck, Europhys. Lett. (to be published).
[9] See, for example, F. E. Christensen, A. Hornstrup, and H. W. Schnopper, Appl. Opt. **27**, 1548 (1988).
[10] S. O. Rice, Commun. Pure Appl. Math. **4**, 351 (1951).
[11] P. Beckmann and A. Spizzichino, *The Scattering of Electromagnetic Waves from Rough Surfaces* (Pergamon, New York, 1963).
[12] P. Croce, J. Opt. **14**, 1 (1983); **14**, 4 (1983).
[13] S. K. Sinha, E. B. Sirota, S. Garoff, and H. B. Stanley, Phys. Rev. B **38**, 2297 (1988).
[14] A. Bruson, C. Dufour, B. George, M. Vergnalt, G. Marchal, and Ph. Mangin, Solid State Commun. **71**, 1045 (1989).
[15] D. E. Savage, J. Kleiner, N. Schimke, Y.-H. Phang, T. Jankowski, J. Jacobs, R. Kariotis, and M. G. Lagally, J. Appl. Phys. **69**, 1411 (1991).
[16] J. B. Kortright, J. Appl. Phys. **70**, 3620 (1991).
[17] O. Renner, M. Kopechy, E. Krousky, F. Shcafers, B. R. Muller, and N. I. Chkhalo, Rev. Sci. Instrum. **63**, 1478 (1992).
[18] J. M. Eastman, in *Physics of Thin Films, Advances in Research and Development*, edited by G. Hass and M. H. Francombe (Academic, New York, 1978), Vol. 10, p. 167.
[19] C. K. Carniglia, Opt. Eng. **18**, 104 (1979).
[20] J. M. Elson, Appl. Opt. **16**, 2872 (1977); J. Opt. Soc. Am. **69**, 48 (1979).
[21] J. M. Elson, J. P. Rahn, and J. M. Bennett, Appl. Opt. **19**, 669 (1980).
[22] P. Bousquet, F. Flory, and P. Roche, J. Opt. Soc. Am. **71**, 1115 (1981).
[23] C. Amra and P. Bousquet, Proc. SPIE **1009**, 82 (1988).
[24] A. I. Erko, D. V. Roshchupkin, A. A. Snigirev, A. M. Smolovich, A. Yu. Nikulin, and G. V. Vereshchagin, Nucl. Instrum. Methods A **282**, 634 (1989).
[25] D. G. Stearns, J. Appl. Phys. **65**, 491 (1989).
[26] J. M. Elson and J. M. Bennett, J. Opt. Soc. Am. **69**, 31 (1979).
[27] E. L. Church, Appl. Opt. **27**, 1518 (1988).
[28] L. G. Parratt, Phys. Rev. **95**, 359 (1954).
[29] M. Born and E. Wolf, *Principles of Optics*, 6th ed. (Pergamon, New York, 1987), p. 51.
[30] T. W. Barbee, Jr., S. Mrowka, and M. C. Hettrick, Appl. Opt. **24**, 883 (1985); D. G. Stearns, R. S. Rosen, and S. P. Vernon, J. Vac. Sci. Technol. A **9**, 2662 (1991).
[31] D. G. Stearns, R. S. Rosen, and S. P. Vernon, Opt. Lett. **16**, 1283 (1991).
[32] J. H. Underwood and T. W. Barbee, Jr., Nature **294**, 429 (1981).
[33] B. K. Agarwal, *X-ray Spectroscopy* (Springer, New York, 1979), p. 137.